Development of a high-affinity peptide that prevents phospholemman (PLM) inhibition of the sodium/calcium exchanger 1 (NCX1)

Pimthanya Wanichawan*†, Kjetil Hodne*†, Tandekile Lubelwana Hafver*†, Marianne Lunde*†, Marita Martinsen*†, William Edward Louch*†, Ole Mathias Sejersted*† and Cathrine Rein Carlson*†[1]

*Institute for Experimental Medical Research, Oslo University Hospital and University of Oslo, Oslo, Norway
†KG Jebsen Cardiac Research Center and Center for Heart Failure Research, University of Oslo, Oslo, Norway

NCX1 (Na^+/Ca^{2+} exchanger 1) is an important regulator of intracellular Ca^{2+} and a potential therapeutic target for brain ischaemia and for diastolic heart failure with preserved ejection fraction. PLM (phospholemman), a substrate for protein kinases A and C, has been suggested to regulate NCX1 activity. However, although several studies have demonstrated that binding of phosphorylated PLM (pSer^{68}-PLM) leads to NCX1 inhibition, other studies have failed to demonstrate a functional interaction of these proteins. In the present study, we aimed to analyse the biological function of the pSer^{68}-PLM–NCX1 interaction by developing high-affinity blocking peptides. PLM was observed to co-fractionate and co-immunoprecipitate with NCX1 in rat left ventricle, and in co-transfected HEK (human embryonic kidney)-293 cells. For the first time, the NCX1–PLM interaction was also demonstrated in the brain. PLM binding sites on NCX1 were mapped to two regions by peptide array assays, containing the previously reported PASKT and QKHPD motifs. Conversely, the two NCX1 regions bound identical sequences in the cytoplasmic domain of PLM, suggesting that NCX1-PASKT and NCX1-QKHPD might bind to each PLM monomer. Using two-dimensional peptide arrays of the native NCX1 sequence KHPDKEIEQLIELANYQVLS revealed that double substitution of tyrosine for positions 1 and 4 (K1Y and D4Y) enhanced pSer^{68}-PLM binding 8-fold. The optimized peptide blocked binding of NCX1-PASKT and NCX1-QKHPD to PLM and reversed PLM(S68D) inhibition of NCX1 activity (both forward and reverse mode) in HEK-293 cells. Altogether our data indicate that PLM interacts directly with NCX1 and inhibits NCX1 activity when phosphorylated at Ser^{68}.

Key words: brain, heart, peptide array, phospholemman, sodium/calcium exchanger.

INTRODUCTION

NCX (Na^+/Ca^{2+} exchanger) is an important regulator of Ca^{2+} homeostasis. It functions as a bidirectional antiporter, exchanging one Ca^{2+} for three Na^+, removing either Ca^{2+} (forward mode) or Na^+ (reverse mode) from the cytosol depending on membrane potential and local ion concentrations [1]. Three different SLC8 (solute carrier 8) genes have been identified in mammals: *SLC8A1* encoding NCX1 [2], *SLC8A2* encoding NCX2 [3], and *SLC8A3*, encoding NCX3 [4,5]. Whereas NCX2 and NCX3 are mainly expressed in brain and skeletal muscle, NCX1 is ubiquitous, being found in virtually all excitable and non-excitable tissues including brain, vascular smooth muscle, kidney and heart. NCX1 is composed of ∼970 amino acids spanning nine TMs (transmembrane segments) and a large cytoplasmic loop between TM5 and TM6. The cytoplasmic loop of NCX1 contains several regulatory domains including the inhibitory XIP (exchanger inhibitory peptide) region which binds to calmodulin [6], two Ca^{2+}-binding domains (CBD1 and CBD2) [7], sites for phosphorylation by PKC (protein kinase C), Ca^{2+}/calmodulin-dependent kinase and tyrosine kinase [8], and reported interaction and cleavage sites for calpain [9] and PLM (phospholemman) [10].

PLM is a 72-amino-acid phosphoprotein belonging to the FXYD1 family of ion transport regulators [11], and it is the first reported endogenous inhibitor of NCX1 [12]. It is highly expressed in brain [13] and heart [14], and has been shown to associate with NCX1 in cardiac membranes [15] and to inhibit NCX1 activity when co-expressed [12,16]. The cytoplasmic region of PLM is reported to interact with PASKT- and QKHPD-containing sequences in the cytoplasmic loop of NCX1 [17] and inhibit NCX1 when it is phosphorylated at Ser^{68} (pSer^{68}-PLM) [18] by PKA (protein kinase A) or PKC. It is well established that PLM phosphorylation relieves its inhibitory effect on NKA (Na^+/K^+-ATPase) [19]. Thus an interesting mechanism is proposed whereby phosphorylation of PLM switches its inhibitory actions from NKA to NCX1 [18]. However, an absence of interaction between PLM and NCX1 has also been reported [20], and it is less clear how PLM regulation of NCX1 is integrated with PLM regulation of NKA [20–22].

A regulatory role for PLM on NCX1 has clear therapeutic potential. NCX1 expression and activity are altered during brain ischaemia, neurodegenerative disorders, aging [23,24] and HF (heart failure). In brain, it has been shown that up-regulation of NCX1 has protective effects during cerebral ischaemia [25], suggesting that inhibition of NCX1 by PLM may be detrimental. Similarly, in heart, increased NCX1 activity is believed to maintain diastolic function in diseases such as HF [26]. Constitutive overexpression of phosphorylated PLM (S68E, mimicking phosphorylated Ser^{68}) in mice was observed to inhibit NCX1 activity, and also resulted in arrhythmia, HF and early mortality [27]. Thus augmenting NCX1 function in disease by

Abbreviations: CBD, calcium-binding domain; CLD, catenin-like domain; DMEM, Dulbecco's modified Eagle's medium; GAPDH, glyceraldehyde-3-phosphate dehydrogenase; HF, heart failure; NCX, Na^+/Ca^{2+} exchanger; HRP, horseradish peroxidase; LV, left ventricle; NKA, Na^+/K^+-ATPase; PKC, protein kinase C; PLM, phospholemman; SLC8, solute carrier 8; TBS-T, TBS with 0.1% Tween 20; TF, trigger factor; TM, transmembrane segment; XIP, exchanger inhibitory peptide.

[1] To whom correspondence should be addressed (email c.r.carlson@medisin.uio.no).

preventing PLM-induced inhibition may serve as a novel strategy for disease treatment in both brain and heart.

In the present study, we aimed to investigate the NCX1–PLM interaction in brain and heart, and analyse the functional consequence of this interaction. First, we mapped the reciprocal PLM–NCX1 binding sites at the amino acid level. Using two-dimensional peptide arrays, we developed further a high-affinity blocking peptide specific for the PLM–NCX1 interaction. Our data demonstrate that the optimized peptide exhibits enhanced affinity for pSer^{68}-PLM and can reverse phosphorylation-dependent PLM inhibition of NCX1.

EXPERIMENTAL

Plasmid DNA

The MGC mouse clone BC079673 (NCX1) was cloned into the first reading frame of pAdTrack-cytomegalovirus (CMV) shuttle vector (plasmid 16405, Addgene). Mouse PLM (AF089734) and PLM mutated at Ser^{68} to an aspartic acid residue (S68D) were cloned with a C-terminal stop codon into pcDNA3.1/myc-HisA (Invitrogen) by Genscript. The fidelity of the cloning and mutation procedures was verified by sequence analysis (Genscript).

Peptide synthesis

Peptides on cellulose membranes were synthesized using Multipep automated peptide synthesizer (standard Fmoc solid-phase peptide synthesis using the SPOT synthesis technique, INTAVIS Bioanalytical Instruments) [28,29]. Parts of the intracellular loop of rat NCX1 (EDM02743) and mouse PLM (Q9Z239) were synthesized as overlapping 20-mer peptides with three amino acid offsets. Peptides in solution were synthesized (listed below) and purified to obtain $>80\,\%$ purity by Genscript. For some of the peptides, a biotin tag was included at the N-terminus. The peptide sequences were: NCX1(229–248), KRYRAGKQRGMIIEHEGDRP; NCX1(235–254), KQRGMIIEHEGDRPASKTEI; NCX1(292–311), ARILKELKQKHPDKEIEQLI; NCX1(301–320), KHPDKEIEQLIELANYQVLS; PLM$_{cyt}$(38–72), KRCRCKFNQQQRTGEPDEEEGTFRSSIRRLSSRRR; pSer^{68}-PLM$_{cyt}$, KRCRCKFNQQQRTGEPDEEEGTFRSSIRRLpSSRRR; NCX1(K301Y,D304Y), YHPYKEIEQLIELANYQVLS; NCX1(301–320) scrambled, VYEKNKLDLLPAIEQEQSHI; NCX1 blocking peptide, CGQPVFRKVHARDHPIPST.

Transfection of HEK-293 cells

HEK (human embryonic kidney)-293 cells were cultured in DMEM (Dulbecco's modified Eagle's medium) (Gibco-BRL) supplemented with 10 % (v/v) FBS (Gibco-BRL), 100 unit/ml penicillin, 0.1 mg/ml streptomycin (penicillin/streptomycin, Sigma–Aldrich) and 1 % non-essential amino acids (Gibco-BRL) and maintained in a 37 °C, 5 % CO_2 humidified incubator. Plasmid DNA was transfected into HEK-293 cells using Lipofectamine™ 2000 (Invitrogen) as instructed by the manufacturer or the $CaCl_2$ method. After 24 h, the cells were lysed in lysis buffer containing 20 mM Hepes, pH 7.5, 150 mM NaCl, 1 mM EDTA and 0.5 % Triton X-100 with Complete™ protease inhibitor cocktail tablets (Complete™ Mini EDTA-free; Roche Diagnostics). For patch-clamp experiments, the 24-h-transfected cells were transferred to poly-L-lysine (Sigma–Aldrich)-coated coverslips and incubated for an additional 24 h in a 37 °C, 5 % CO_2 humidified incubator.

Preparation of rat left ventricle and brain lysate

Frozen mouse brain or LV (left ventricle) from rats was pulverized in a mortar with liquid nitrogen, followed by addition of ice-cold lysis buffer (20 mM Hepes, pH 7.5, 150 mM NaCl, 1 mM EDTA and 0.5 % Triton) supplemented with 1 mM PMSF (Sigma–Aldrich) and Complete™ protease inhibitor cocktail tablets. Tissue samples were homogenized three times for 1 min on ice with a Polytron 1200 and centrifuged at 100 000 ***g*** for 60 min at 4 °C. Supernatants were collected and stored at − 70 °C.

Fractionation

Rat LV and cardiomyocytes were fractionated using a Compartment Protein Extraction Kit (Millipore) according to the manufacturer's instructions.

Neonatal rat cardiomyocytes

Animals were handled according to the National Regulations on Animal Experimentation in accordance with the Norwegian Animal Welfare Act. The animal experiments were approved by the Norwegian National Animal Research Committee, which conforms to the Guide for the Care and use of Laboratory Animals published by the U.S. National Institutes of Health (NIH publication number 85-23, revised 1996). Neonatal cardiomyocytes were prepared from the LV of 1–3-day-old Wistar rats as described previously [9]. The cardiomyocytes were incubated in a plating medium consisting of DMEM (Sigma–Aldrich), M-199 (Sigma–Aldrich), penicillin/streptomycin (Sigma–Aldrich), horse serum (BioWhittaker) and FBS (BioWhittaker) in a humidified incubator with 5 % CO_2 at 37 °C for 24 h before protein fractionation.

Overlay assay

Synthesized peptide membranes were first activated by soaking membranes in methanol for a few seconds and were then washed three times for 10 min with TBS-T (TBS with 0.1 % Tween 20). The membranes were then incubated with blocking solution (1 % casein) (Roche Diagnostics) at room temperature. After 1 h of blocking, the membranes were incubated with 1–5 μM biotinylated peptide in 1 % casein overnight at 4 °C with gentle agitation. For the competition experiments, the blocking peptide [5 μM NCX1(K301Y,D304Y)] was pre-incubated with the membranes overnight at 4 °C with gentle agitation, before incubation with biotinylated peptide for 2 h. The membranes were then washed three times for 10 min with TBS-T. Binding was detected by immunoblotting. The peptides are covalently linked to the membrane and should, according to the manufacturer (Intavis), remain on the membrane after washing and stripping protocols.

Pull-down assay with biotinylated peptides

Each biotinylated peptide (8 μM) was incubated with 25 μl of monoclonal anti-biotin antibody-conjugated beads (A-1559, Sigma–Aldrich) in 100 μl of PBS for 2 h at 4 °C with rotation. To remove unbound peptide, the beads were washed three times with PBS, followed by adding 100 μl of HEK-293 cell lysates, 0.5 μg of recombinant His–TF (trigger factor)–NCX1$_{cyt}$ or 133 μM PLM$_{cyt}$ peptide diluted in 150 μl of immunoprecipitation buffer containing 1 % (w/v) BSA. The samples were rotated for 2 h at 4 °C followed by washing the beads three times with immunoprecipitation buffer (20 mM Hepes, pH 7.5, 150 mM

NaCl, 1 mM EDTA and 1 % Triton X-100) before boiling in 2× SDS loading buffer. Binding was analysed by immunoblotting.

Immunoprecipitation

Immunoprecipitation was performed by incubating 2 μg of the appropriate antibody with 200 μl of protein sample [rat heart lysates (6.7 μg/μl), HEK-293 lysates (10 μg/μl) or brain lysate (1.5 μg/μl)] and Protein A/G PLUS–agarose (Santa Cruz Biotechnology) overnight at 4 °C with rotation. The next day, samples were washed three times in immunoprecipitation buffer (or PBS for brain) and boiled in 2× SDS loading buffer before SDS/PAGE analysis. An equal amount of rabbit IgG (sc-2027, Santa Cruz Biotechnology) was used as a negative control. Blocking peptide (antigen: cardiac NCX1, sequence: CGQPVFRKVHARDHPIPST) (Genscript) was incubated with anti-NCX1 before immunoprecipitation (negative control). Usually 20 μl of the protein sample was used as an input control.

Immunoblotting

Samples from pull-down assays were analysed by SDS/PAGE on 4–15 % or 15 % Criterion Tris/HCl gels (Bio-Rad Laboratories) and blotted on to PVDF membranes (GE Healthcare). The PVDF membranes and peptide arrays were blocked in 5 % (w/v) dried non-fat skimmed milk powder or 1 % (w/v) casein in TBS-T for 60 min at room temperature and incubated overnight with primary antibody at 4 °C. After incubation with primary antibody, the membranes were washed five times for 5 min in TBS-T and incubated further with an HRP (horseradish peroxidase)-conjugated secondary antibody. The membranes were developed using ECL Plus (GE Healthcare). The chemiluminescence signals were detected using a LAS 1000 or LAS 4000 instrument (Fujifilm).

Antibodies and recombinant protein

Anti-NCX1 (epitope: GQPVFRKVHARDHPIPST) was custom-made by Genscript. HRP-conjugated anti-biotin (A0185) was purchased from Sigma–Aldrich. Anti-PLM (anti-FXYD1) (ab76597) was purchased from Abcam. Anti-GAPDH (glyceraldehyde-3-phosphate dehydrogenase) (V-18) (sc-20357) was obtained from Santa Cruz Biotechnology. Anti-calsequestrin (PA1-913) was from Thermo Scientific. HRP-conjugated anti-rabbit IgG (NA934V, GE Healthcare) and HRP-conjugated anti-goat IgG (HAF109, R&D Systems) were used as secondary antibodies. Recombinant cytoplasmic NCX1 protein (His–TF–$NCX1_{cyt}$) with an N-terminal His and TF tag to stabilize the protein was custom-made by Genscript.

Patch-clamp experiments

Whole-cell patch-clamp experiments were conducted on NCX1- and PLM(S68D)-transfected HEK-293 cells. The patch electrodes were made from borosilicate glass with filament, and had a final resistance between 2 and 4 MΩ. The electrodes were connected to an Axoclamp 200B amplifier and a Digidata 1550, controlled by pClamp 10.2 software (all from Axon Instruments/Molecular Devices). The recorded signals were sampled at 20 kHz, filtered at 2 kHz using an analogue low-pass Bessel filter, and stored on the computer. The recordings were performed at 37 °C in an extracellular solution containing 140 mM NaCl, 5 mM CsCl, 1.2 mM $MgSO_4$, 1.2 mM NaH_2PO_4, 5 mM $CaCl_2$, 10 mM Hepes and 10 mM glucose (pH 7.4 with CsOH) and osmolality 290 mOsm. To block K^+-, Ca^{2+}-, Cl^-- and Na^+/K^+-ATPase currents, we used caesium, 20 μM nifedipine, 30 μM niflumic acid and 1 mM ouabain. The patch pipettes were filled with a solution containing 100 mM caesium glutamate, 1 mM MgCl, 10 mM Hepes, 4 mM NaCl, 2.5 mM Na_2-ATP, 10 mM EGTA and 6 mM $CaCl_2$ (pH 7.2) and osmolality 270 mOsm. In experiments to assess the effect of the optimized peptide we added 5 μM of either optimized or scrambled control peptide to the internal solution. Recordings were corrected for liquid junction potential (15 mV), calculated using pCLAMP 10 software ($V_{membrane} = V_{pipette} - 15$ mV). Following whole-cell configuration, the series resistance, seal resistance and cell capacitance were monitored throughout the experiment. Only cells with a stable gigaseal and cell capacitance were used. In addition, we only used cells with series resistance <10 MΩ. The cells were clamped to −43 mV (reversal potential) for 6 min to allow sufficient intracellular diffusion of both ions and peptides. The NCX1 current was elicited by a descending voltage ramp from 120 mV to −100 mV and isolated using 5 μM Ni^{2+}. The currents were normalized to cell capacitance and the current (I)–voltage (V) relationships were plotted from −100 to 100 mV.

Densitometric analysis

Densitometric analysis was performed using Image Gauge version 4.0, ImageQuant TL (GE Healthcare) or ImageJ (NIH).

Statistics

All data are expressed as means ± S.E.M. Comparisons between two groups were analysed using unpaired Student's t test (GraphPad Prism 5.04). $P < 0.05$ was considered statistically significant.

RESULTS

Identification of the PLM–NCX1 interaction in heart, brain and HEK-293 cells

Several experiments were performed to investigate the PLM–NCX1 interaction. First, PLM was observed together with NCX1 in membrane fractions isolated from rat neonatal cardiomyocytes (Figure 1A, left-hand panel) and rat LV (Figure 1A, right-hand panel) using specific anti-PLM (epitope mapped in Figure 1B) and anti-NCX1 antibodies [30]. Secondly, immunoprecipitation of endogenous NCX1 using anti-NCX1 antibodies identified co-precipitation of endogenous PLM in both rat LV and brain lysate (Figures 1C and 1D respectively). Moreover, immunoprecipitation of NCX1 expressed in HEK-293 cells co-transfected with PLM revealed co-precipitation of PLM (Figure 1E). NCX1 precipitated PLM(S68D) (mimicking phosphorylated PLM) and unphosphorylated PLM (Figure 1F) at similar levels. Finally, pull-down assays with biotinylated peptides consisting of the cytoplasmic part of PLM or $pSer^{68}$-PLM (Figure 1G, schematic representation in the upper panel, immunoblots shown in the lower panel) and recombinant His–TF–$NCX1_{cyt}$ were performed with anti-biotin–agarose. His–TF–$NCX1_{cyt}$ precipitated with both PLM(38–72) and $pSer^{68}$-PLM(38–72) (Figure 1H), confirming that the cytoplasmic domain of PLM binds directly to the NCX1 cytoplasmic loop, and verifying that this interaction is independent of the phosphorylation status of Ser^{68} on PLM. Sequence alignments show that the PLM cytoplasmic domain is identical in human, rat, mouse, pig and

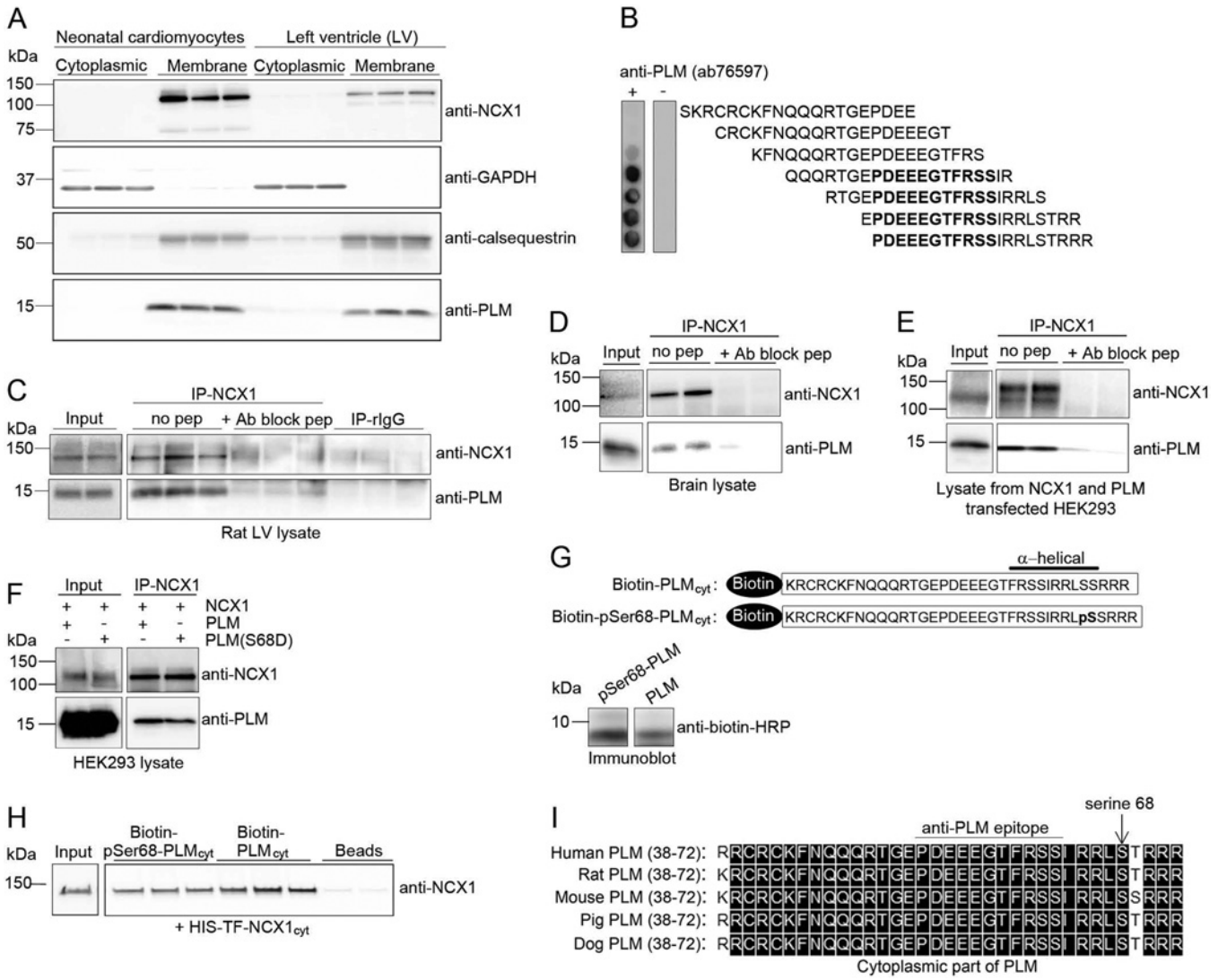

Figure 1 Confirmation of a direct PLM–NCX1 interaction

(**A**) NCX1 and PLM were analysed in cytoplasmic and membrane fractions isolated from rat neonatal cardiomyocytes and LV using anti-NCX1 and anti-PLM antibodies. GAPDH and calsequestrin were used as controls for cytoplasmic and membrane fractions respectively. (**B**) Epitope mapping was performed by overlaying an array of immobilized overlapping 20-mer PLM peptides with anti-PLM (ab76597, left-hand panel). Amino acids in bold were relevant for anti-PLM binding. Immunoblotting without anti-PLM was used as a negative control (right-hand panel). (**C**) Rat LV, (**D**) brain or (**E** and **F**) lysate from HEK-293 cells co-transfected with NCX1 and PLM or PLM(S68D) was subjected to immunoprecipitation using anti-NCX1. Immunoprecipitates and lysate was immunoblotted with anti-NCX1 and anti-PLM antibodies. A specific anti-NCX1 blocking peptide and non-relevant rabbit IgG were used as negative controls. (**G**) Schematic presentation of biotinylated peptides covering PLM_{cyt} and $pSer^{68}$-PLM_{cyt} (upper panel). The α-helical region is indicated. Immunoblotting analysis of the two biotinylated peptides using HRP-conjugated anti-biotin is shown in the lower panel. (**H**) Pull-down assay with biotin–PLM_{cyt} and biotin–$pSer^{68}$-PLM_{cyt} against recombinant His–TF–$NCX1_{cyt}$ (containing the cytoplasmic part of NCX1) using monoclonal anti-biotin-conjugated beads. Pull-down of NCX1 was analysed by immunoblotting using anti-NCX1. (**I**) Alignment of the cytoplasmic part of PLM in human, rat, mouse, pig and dog. Black boxes indicate the identical amino acids (DNA Star). Molecular masses are indicated in kDa. Ab, antibody; IP, immunoprecipitation; pep, peptide; Ab block pep, anti-NCX1 blocking peptide.

dog, with the exception of a serine residue at position 69 in mouse (Figure 1I).

Identification of the reciprocal PLM–NCX1 binding sites

To map PLM-binding sites in NCX1 more precisely, 20-mer NCX1 peptides were overlaid with biotin–PLM_{cyt} and biotin–$pSer^{68}$-PLM_{cyt} peptides. Both peptides bound to PASKT- and QKHPD-containing sequences in NCX1 (Figures 2A and 2B, marked in bold letters), consistent with a previous study [31]. In addition, both peptides bound to the inhibitory XIP region in NCX1 [6] (Figures 2A and 2B, underlined sequences) and to a region C-terminal of the QKHPD motif (T^{366}RLMTGAGNILKRHAADQAR^{385}). As peptide array screening is semi-quantitative, quantitative analysis with selected peptides in solution should be performed. Thus four peptides covering amino acids 229–248, 235–254, 292–311 and 301–320 in NCX1 (black arrows in Figures 2A and 2B) were also synthesized as purified biotinylated peptides in solution (sequences given in Figure 2C). These NCX1 peptides were analysed further for their binding affinity to PLM expressed in HEK-293 cells. Pull-down assays using anti-biotin-conjugated beads and immunoblotting with anti-PLM revealed that all four NCX1 peptides precipitated similar levels of PLM (Figure 2D).

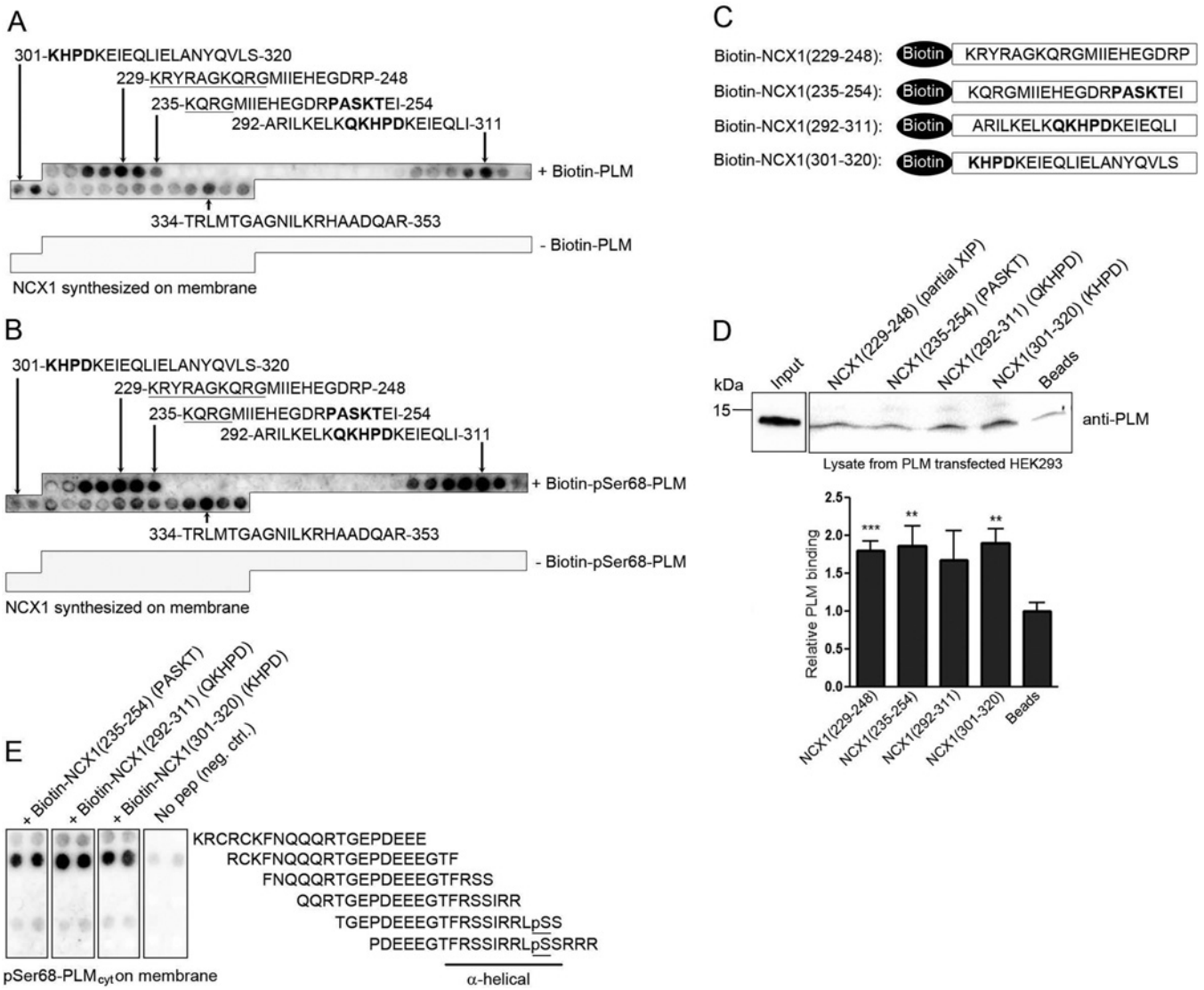

Figure 2 Identification of pSer^{68}-PLM/PLM binding in the cytoplasmic part of NCX1

(**A**) Biotin–PLM and (**B**) biotin–pSer^{68}-PLM binding was identified by overlaying the peptides on membranes containing 20-mer overlapping NCX1 peptides, followed by immunoblotting using HRP-conjugated anti-biotin (upper panels). The PLM-binding residues, PASKT and QKHPD, identified by Zhang et al. [31] are marked in bold. Underlined amino acids indicate the XIP region. Arrows indicate the four sequences that were investigated further. Membranes incubated with only HRP-conjugated anti-biotin were used as negative controls (lower panels in **A** and **B**). (**C**) Schematic illustration of the four biotinylated NCX1 peptides used in the pull-down assay. (**D**) Pull-down assay with the biotinylated NCX1 peptides against PLM expressed in HEK-293 cells. PLM binding was analysed by immunoblotting using anti-PLM (upper panel). Beads were used as a negative control. Molecular mass is indicated in kDa. A bar graph shows the relative PLM binding quantified by densitometry analysis. Differences were analysed using unpaired Student's t test (**$P < 0.01$, *** $P < 0.001$) ($n = 4$–7). Results are means $\pm$ S.E.M. (**E**) Biotin–NCX1(235–254) (PASKT), biotin–NCX1(292–311) (QKHPD) and biotin–NCX1(301–320) (KHPD) binding was identified by overlaying the peptides on membranes containing 20-mer overlapping pSer^{68}-PLM peptides, followed by immunoblotting using HRP-conjugated anti-biotin. Phosphorylated Ser^{68} is underlined. The C-terminal α-helical region is indicated. Negative controls were performed by omitting incubation of the biotinylated peptides with the membranes (right-hand panels).

To map where the NCX1-PASKT- and NCX1-QKHPD-containing sequences bound in PLM, biotinylated peptides containing the two motifs (the three lowermost peptides in Figure 2C) were overlaid on the pSer^{68}-PLM cytoplasmic part synthesized as 20-mer overlapping peptides on membranes. Binding was detected by using HRP-conjugated anti-biotin antibody. The results revealed that all three NCX1 peptides bound strongest to RCKFNQQQRTGEPDEEEGTF (Figure 2E), consistent with NCX1 binding being independent of Ser^{68} phosphorylation in PLM. RCKFNQQQRTGEPDEEEGTF covers the more flexible PLM region, upstream of the α-helical region (Figure 2E).

Optimization of PLM-binding sequences by two-dimensional peptide arrays

The two uppermost peptides in Figure 2(C) were excluded for optimization as they contain the autoregulatory domain of NCX1 (XIP), which is known to bind NCX1 and calmodulin [6]. The two lowermost sequences were optimized further by two-dimensional peptide arrays, where each amino acid in the native peptide sequences was systemically replaced with every possible amino acid. Immunoblotting using HRP-conjugated anti-biotin showed that substitutions within NCX1(301–320) (KHPDKEIEQLIELANYQVLS) strongly increased binding to

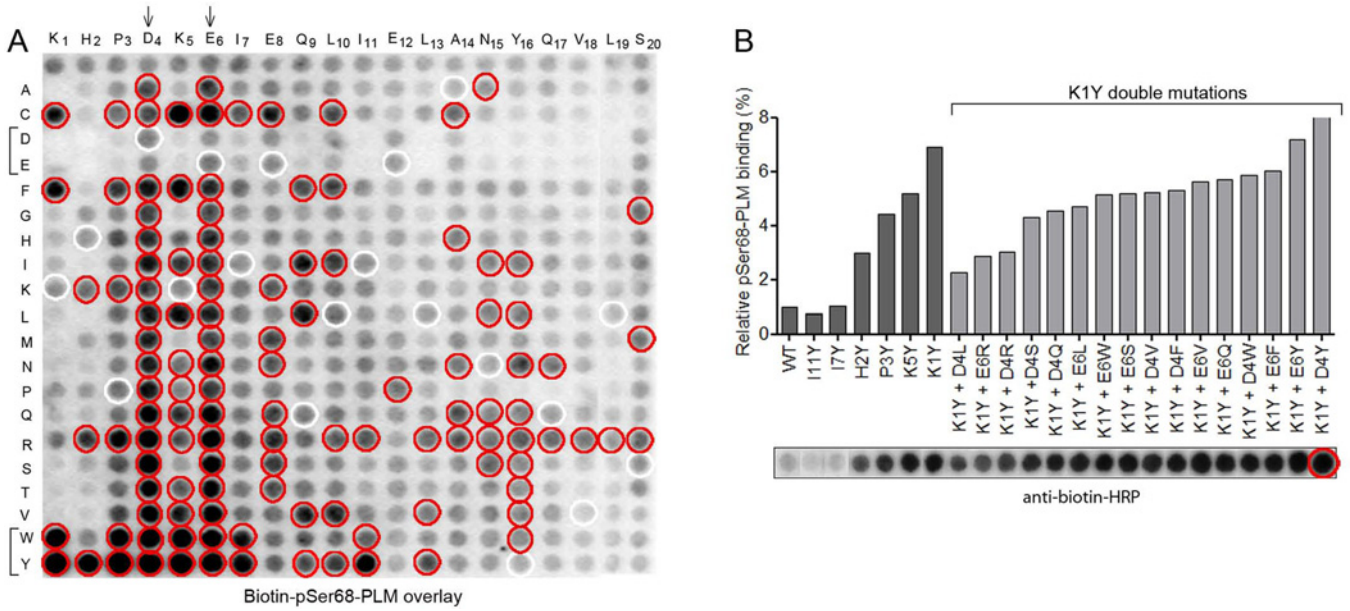

Figure 3 Optimization of pSer^{68}-PLM binding sequences

(**A**) A two-dimensional peptide array of NCX1(301–320) (KHPDKEIEQLIELANYQVLS) was synthesized and overlaid with biotin–pSer^{68}-PLM. The binding was detected by using HRP-conjugated anti-biotin. Each residue in the native NCX1 sequence is written as a single-letter code above the array, whereas substitutions are given as single-letter codes to the left (vertically). The first row of the array shows pSer^{68}-PLM binding to the native NCX1(301–320) sequence. White circles indicate internal control peptides of the native NCX1 sequence within the array. Red circles indicate substitutions that enhanced pSer^{68}-PLM binding. Arrows above the array indicate the flexible positions 4 and 6 in the native peptide sequence. The representative data were acquired from two independent experiments. NCX1 numbering excludes the signal peptide at N-terminus. (**B**) Biotin–pSer^{68}-PLM binding to single- and double-substituted NCX1(301–320) was analysed by immunoblotting using HRP-conjugated anti-biotin (lower panel). Relative pSer^{68}-PLM binding was quantified by densitometry analysis (upper panel). The presented data are averages from two independent experiments. The red circle indicates the final optimized peptide in (**B**).

biotin–pSer^{68}-PLM (Figure 3A). This effect was not observed in NCX1(292–311) (ARILKELKQKHPDKEIEQLI) (results not shown). The pSer^{68}-PLM binding affinity was dramatically increased when NCX1(301–320) (KHPDKEIEQLIELANYQVLS) was replaced at positions 1–11 (labelled with red circles) compared with internal control peptides (white circles). Especially, tryptophan and tyrosine substitutions highly increased the affinity for pSer^{68}-PLM (Figure 3A, lower bracket on the left). Replacing with negatively charged amino acids such as aspartic acid and glutamic acid were not favourable, as they mostly reduced or abolished pSer^{68}-PLM binding (Figure 3A, upper bracket on the left). Consistent with the disfavour for negatively charged amino acids, removal of the endogenous aspartic acid in position 4 (D4) and glutamic acid in position 6 (E6) mostly increased pSer^{68}-PLM binding (indicated with arrows above the array in Figure 3A).

In a second peptide membrane synthesis, residues of the native NCX1(301–320) peptide sequence were individually replaced with tyrosine at position 1 (K1), 2 (H2), 3 (P3), 5 (K5), 7 (I7) or 11 (I11). Immunoblotting using HRP-conjugated anti-biotin revealed that K1Y, H2Y, P3Y and K5Y greatly increased the pSer^{68}-PLM affinity (Figure 3B). In an attempt to increase the affinity to an even higher level, double substitutions in the NCX1(301–320) sequence were performed. Each of the single mutations, i.e. K1Y, H2Y, P3Y, K5Y, I7Y and I11Y, was combined with amino acid substitutions in the more flexible positions D4 and E6 (indicated by arrows above the array in Figure 3A). Most of the double-substituted peptides showed increased pSer^{68}-PLM binding compared with the native NCX1 peptide (average data from two independent experiments are shown only for K1Y double mutations in Figure 3B). In conclusion, the double mutation K1Y, D4Y had the highest affinity for pSer^{68}-PLM (Figure 3B, labelled in red circle). K1 and D4 correspond to Lys^{301} and Asp^{304} in the full-length NCX1 protein.

The optimized peptide binds strongly to pSer^{68}-PLM and blocks binding of NCX1-PASKT and NCX1-KHPD

Pull-down experiments using biotinylated peptides covering the native NCX1(301–320) sequence, the optimized sequence (Opt-pep) or a scrambled sequence (sequences are given in Figure 4A), together with an untagged PLM$_{cyt}$ peptide, were performed. Immunoblotting with anti-PLM showed that Opt-pep bound more strongly to PLM$_{cyt}$ than native NCX1(301–320) peptide (Figure 4B). The scrambled peptide and beads without any peptide were used as negative controls. In addition to stronger binding, overlay assays indicated that Opt-pep also bound more broadly to pSer^{68}-PLM sequences synthesized on membranes (Figure 4C, middle panels), compared with native NCX1(301–320) peptide (Figure 4C, left-hand panels).

To test whether Opt-pep was able to block NCX1 binding, untagged Opt-pep was pre-incubated with pSer^{68}-PLM$_{cyt}$ synthesized on membranes, before overlaying with biotin–NCX1(235–254) (containing the PASKT motif) and biotin–NCX1(301–320) (containing the KHPD motif). Immunoblotting with HRP-conjugated anti-biotin showed that Opt-pep efficiently blocked binding of both NCX1 peptides to pSer^{68}-PLM (middle panels in Figures 4D and 4E respectively). Altogether, our data indicate that Opt-pep effectively blocks the NCX1–PLM interaction.

Sequence alignments show that the native NCX1 sequence KHPDKEIEQLIELANYQVLS and surrounding regions were almost identical in human, rat, mouse and dog, suggesting that

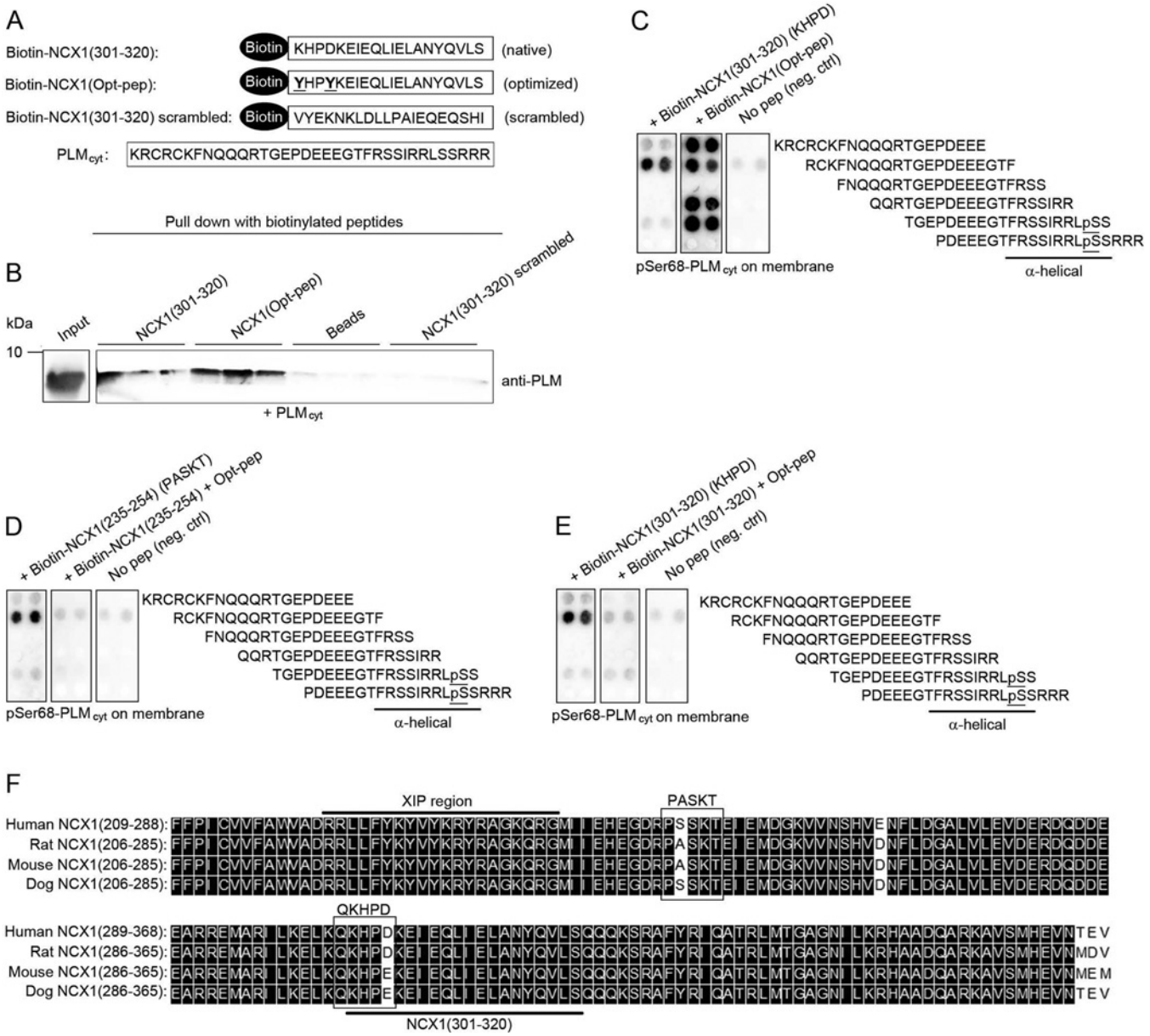

Figure 4 Analyses of the optimized peptide sequence (Opt-pep)

(**A**) Schematic illustration of biotin–NCX1(301–320) (native sequence), biotin–NCX1(Opt-pep) (optimized peptide sequence), biotin–NCX1(301–320) scrambled (control sequence) and an untagged PLM_{cyt} peptide used in pull-down assay in (**B**). (**B**) Pull-down assays with biotin–NCX1(301–320) and biotin–NCX1(Opt-pep) against the untagged PLM_{cyt} peptide. PLM binding was analysed by immunoblotting using anti-PLM. A biotin–NCX1(301–320) scrambled peptide and beads were used as negative controls. (**C**) Binding of biotin–NCX1(301–320) and biotin–NCX1(Opt-pep) was identified by overlaying the peptides on membranes containing 20-mer overlapping $pSer^{68}$-PLM peptides, followed by immunoblotting using HRP-conjugated anti-biotin. Binding of (**D**) biotin–NCX1(235–254) and (**E**) biotin–NCX1(301–320) to $pSer^{68}$-PLM with or without a pre-incubation of Opt-pep. Binding was analysed by immunoblotting using HRP-conjugated anti-biotin. Phosphorylated Ser^{68} is underlined and the C-terminal α-helical region is indicated in (**C**)–(**E**). Incubation with only HRP-conjugated anti-biotin (omitting incubation with the peptides) was used as negative control (right-hand panels in **C**–**E**). (**F**) Alignment of human, rat, mouse and dog NCX1 sequence. Position of the XIP region and the native NCX1 sequence (amino acids 301–320) used for optimization are underlined. Black boxes indicate identical amino acids (DNA Star).

Opt-pep is able to block the NCX1–PLM interaction across species (Figure 4F).

Opt-pep reverses PLM(S68D) inhibition of NCX1 activity

To study the effect of Opt-pep on NCX1 current in the presence of $pSer^{68}$-PLM, we transfected HEK-293 cells with NCX1 and PLM(S68D) (mimicking phosphorylated PLM). The currents were recorded in a whole-cell patch-clamp configuration during voltage ramps from 120 to -100 mV. Typical recordings of current traces are shown in Figures 5(A) and 5(B), with either 5 μM Opt-pep or 5 μM scrambled peptide included in the internal pipette solution respectively. Notably, the Opt-pep gradually relieved PLM induced NCX1 inhibition with the full effect observed after ~5 min of dialysis [Figure 5A, dark grey (3 min) and black (5 min) traces]. This gradual increase in current was not observed using scrambled peptide (Figure 5B). Following 5 min of dialysis, the extracellular recording solution perfusing the cells was changed to a solution containing 5 μM Ni^{+} (Figures 5A

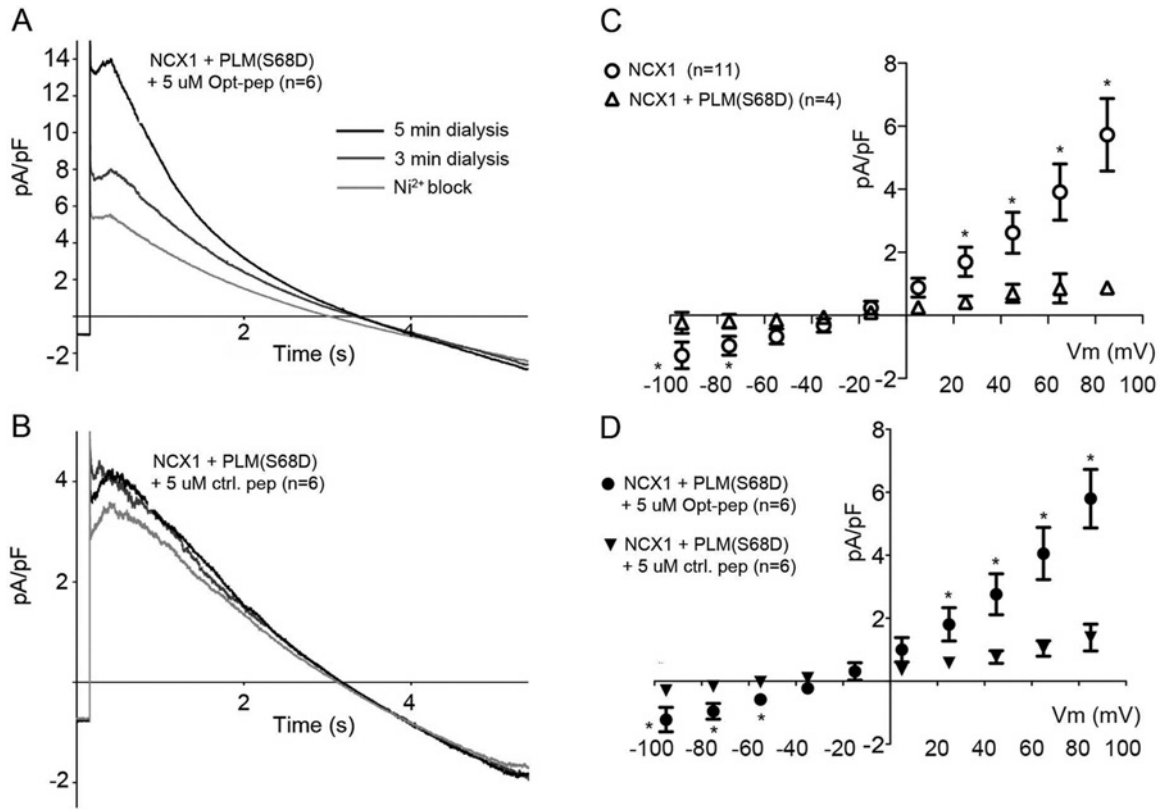

Figure 5 Opt-pep reverses PLM(S68D) inhibition of NCX1

Whole-cell patch-clamp recordings from transfected HEK-293 cells. The different current traces were evoked using a voltage ramp from 120 to -100 mV. (**A**) Recordings of current traces with 5 μM Opt-pep or (**B**) 5 μM scrambled peptide added to the pipette. All currents were normalized to the cell capacitance (pA/pF). (**C** and **D**) The Ni^{2+}-sensitive currents were plotted on a *I–V* curve with the ordinate showing normalized current and the abscissa showing the voltage in mV. NCX1 alone (open circles, $n = 11$) and NCX1 co-expressed with PLM(S68D) (open triangles, $n = 4$) are shown in (**C**), whereas NCX1 co-expressed with PLM(S68D) and 5 μM Opt-pep added (closed circles, $n = 6$), and NCX1 co-expressed with PLM(S68D) and 5 μM scrambled control peptide added (closed inverted triangles, $n = 6$) are shown in (**D**) (Student's *t* test, $^*P < 0.05$).

and 5B, light grey trace) The subtracted Ni^{2+}-sensitive currents, corresponding to the NCX1 current, were plotted as an *I–V* curve from -100 to 100 mV (Figures 5C and 5D). The assays to measure the effect of PLM(S68D) were first validated without the presence of Opt-pep. The normal NCX1 (Figure 5C, open circles) exhibited current in both forward and reverse modes. Consistent with the literature [12], co-transfecting NCX1 with PLM(S68D) inhibited both forward- and reverse-mode current (Figure 5C, open triangles). However, the presence of Opt-pep relieved the PLM inhibition (Figure 5D, closed circles) and the NCX1 current returned to the range observed in NCX1 transfected cells without PLM(S68D). The presence of the scrambled control peptide (sequence given in Figure 4A) did not relieve the inhibition of phosphorylated PLM (closed inverted triangles), strongly indicating that the reversal of NCX1 inhibition was sequence-specific.

A model of the functional interaction of $pSer^{68}$-PLM with NCX1 (inhibition) and relief of its inhibition by Opt-pep is shown in Figure 6.

DISCUSSION

Although there have been several studies suggesting that PLM is an endogenous NCX1 inhibitor in heart [32], another study has shown no direct interaction between the two proteins [20]. In the present study, we confirm that PLM interacts directly with NCX1 and that PLM phosphorylation at Ser^{68} inhibits NCX1 activity. We observed that PLM precipitated with NCX1 expressed in HEK-293 cells and in rat LV lysates [12,16], and demonstrated for the first time that PLM and NCX1 also interact in the brain. We found that the cytoplasmic domain of PLM binds directly to PASKT- and QKHPD-containing sequences in the NCX1 cytoplasmic loop, as reported previously [17,31]. This interaction was observed to be independent of Ser^{68} phosphorylation. Finally, we developed a blocking peptide specific for the PLM–NCX1 interaction, which reversed the inhibitory effect of PLM(S68D) on NCX1 activity in HEK-293 cells.

Mapping of PLM–NCX1 reciprocal binding sites

By extensive use of peptide array technology, we mapped PLM binding to two regions in NCX1, containing the PASKT and QKHPD motifs, reported previously to be involved in PLM binding [17]. PLM also bound to the XIP domain, which is in close proximity to PASKT. The XIP domain, containing a calmodulin-binding site [33], has an autoregulatory role in regulating NCX1 activity [6] and is involved in Na^+-dependent inactivation [34]. However, PLM also inhibits NCX1 when the XIP region is deleted [17]. Importantly, the PLM-binding region in NCX1 overlapped with the YFP cloning site in the FRET study finding no PLM–CFP–NCX1–YFP interaction [20].

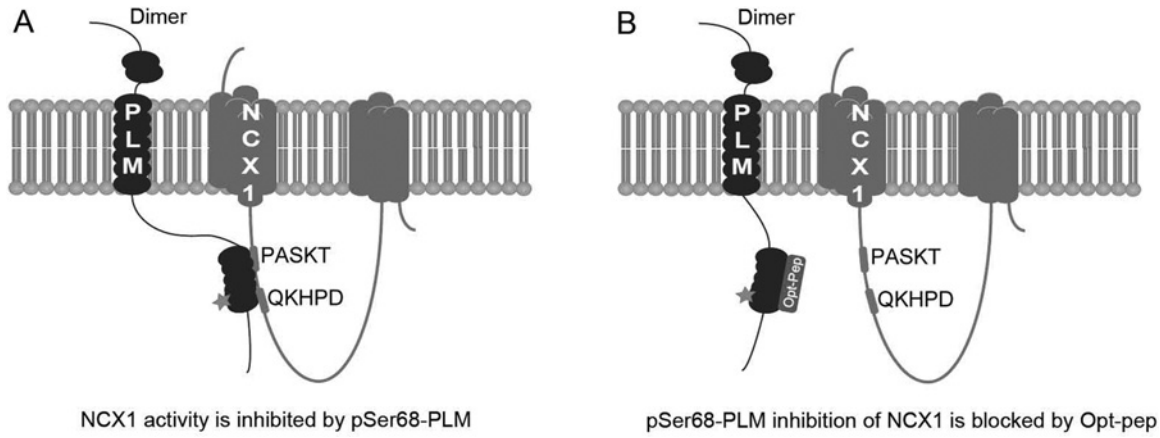

Figure 6 A schematic model of PLM(S68D) inhibition of NCX1 activity and relief of its inhibition by Opt-pep

(**A**) pSer^{68}-PLM (phosphorylation denoted with a star) dimer binds to the cytoplasmic loop of NCX1 and inhibits NCX1 activity [16,18]. (**B**) Opt-pep binds to cytoplasmic PLM and relieves the inhibitory effect of pSer^{68}-PLM on NCX1. The stoichiometry of the PLM–NCX1 interaction is unknown.

NCX-PASKT and NCX1-QKHPD bound to R^{41}CKFNQQQRTGEPDEEEGTF^{60} in PLM$_{cyt}$. Thus NCX1 binding resided outside Ser^{63}, Ser^{68} and Thr^{69} in PLM, confirming that the PLM–NCX1 interaction is not dependent on PLM phosphorylation. The finding of identical binding motifs suggests that NCX-PASKT and NCX1-QKHPD might bind to each monomer in the PLM dimer. The two motifs are important for NCX1 regulation, because alanine mutations in these two motifs are reported to abolish or reduce NCX1 inhibition. Alanine mutation of lysine in the QKHPD motif (Q**A**HPD) removes PLM inhibition of NCX1 [31]. Consistently, pSer^{68}-PLM was not able to bind to NCX1(301–320), when the lysine residue at position 301 was mutated to alanine (**A**HPDKEIEQLIELANYQVLS) (Figure 3A). Importantly, the NCX1-binding site in PLM (R^{41}CKFNQQQRTGEPDEEEGTF^{60}) overlapped with the PLM antibody epitope (ab76597) (Figure 1B). Thus the antibody will only precipitate PLM without NCX1 bound, causing a false negative result.

The NCX-PASKT and NCX1-QKHPD motifs are located within an unstructured domain of NCX1 (CLD or catenin-like domain). The CLD is suggested to be important for transducing signals from CBD1 and CBD2 in NCX1 to the TMs upon Ca^{2+} binding [35]. It is less likely that PLM inhibits Ca^{2+}-dependent activation of NCX1, since PLM inhibits NCX1 even in the absence of the CBDs [10], and also inhibits the NCX1-G503P mutant which lacks Ca^{2+}-dependent activation of NCX1 [36]. Rather, it has been suggested that PLM regulates NCX1 activity by altering the oligomerization state of NCX1 [31]. Experiments using chemical cross-linking [37] and FRET [38] have suggested that NCX1 exists as dimers in the cell membrane of insect and *Xenopus* oocytes. Further experiments are required to investigate whether the NCX-PASKT and NCX1-QKHPD motifs are held distant or in close proximity in the NCX1 monomer or in a possible dimer. The stoichiometry of the PLM–NCX1 interaction is unknown.

Development of an NCX1–PLM blocking peptide (Opt-pep)

The blocking peptide was derived from a NCX1 sequence containing the partial QKHPD motif [31]. Optimization of the NCX1-derived sequence by two-dimensional peptide arrays identified amino acids important for increased pSer^{68}-PLM$_{cyt}$ binding. These specific amino acids were therefore replaced in the peptide sequence. The final optimized peptide (Opt-pep), where tyrosine substituted for lysine and aspartic acid (**Y**HP**Y**KEIEQLIELANYQVLS), had an 8-fold higher affinity for pSer^{68}-PLM$_{cyt}$ compared with the native NCX1 sequence. Opt-pep blocked binding of NCX1-PASKT and NCX1-QKHPD to PLM and reversed the inhibitory effect of PLM(S68D) on NCX1 activity (both forward and reverse modes) in HEK-293 cells. The reversal was specific because a scrambled control peptide had no effect.

Will Opt-pep interfere with the NKA–PLM interaction?

PLM regulates NCX1 and NKA differently. The cytoplasmic domain in the PLM dimer binds to NCX1, whereas the transmembrane domain in the PLM monomer binds to the NKA α-subunit. Contrary to NCX1 regulation, phosphorylation at Ser^{68} relieves its inhibitory effect on NKAα [32], although pSer^{68}-PLM still remains physically associated [20,39]. Two PLM–NKAα interaction sites have been reported [40]. PLM-Phe^{28} and NKA-Glu^{960} have been reported to be critical for the inhibitory interaction. A second non-regulatory NKA interaction site is suggested in the N-terminus (extracellular) or in the transmembrane domain of PLM. Thus, since Opt-pep binds to the cytoplasmic part of PLM, it is less likely that Opt-pep will interfere with the PLM–NKA interaction. PLM has also been suggested to modulate the activity of L-type Ca^{2+} channels in heterologous expression systems [41,42] and in adult cardiac myocytes [43]. Interestingly, only the extracellular and the transmembrane domains of PLM were found to be crucial for modulation of L-type Ca^{2+} channel, suggesting that Opt-pep will not interfere with the L-type Ca^{2+} channel activity.

Will increased NCX1 activity be beneficial in HF and brain ischaemia?

PLM is considered to be a stress protein [32]. Under resting conditions, PLM is functionally quiescent, and the *in vivo* myocardial contractility is similar between wild-type and PLM-knockout mice [32,44]. However, during catecholamine stress, when PLM is phosphorylated, one of its major physiological functions is to suppress Na^+ overload through NKA activation.

Low intracellular Na^+ levels favour Ca^{2+} extrusion by NCX1, its 'forward' mode of operation. However, such indirect effects of catecholaminergic stress on Ca^{2+} extrusion appear to be tempered by direct inhibition of NCX1 activity upon binding of $pSer^{68}$-PLM. Thus the net effects of PLM on cardiomyocyte Ca^{2+} handling and contraction/relaxation are complex, particularly since experimental data indicate that NKA sets local gradients of Na^+, which regulate NCX1 activity [45,46]. This insight suggests that therapeutic modulation of PLM levels may be less appropriate than modulation of PLM interaction with either NKA or NCX. Our data indicate that blockade of the interaction between $pSer^{68}$-PLM and NCX1 increases NCX1 activity. Since NCX1 competes with SERCA (sarcoplasmic/endoplasmic reticulum Ca^{2+}-ATPase), an increase in NCX1 activity has been shown to reduce sarcoplasmic reticulum Ca^{2+} content and thus reduce contractility [47]. Thus inhibition of the $pSer^{68}$-PLM–NCX1 interaction would not be expected to be beneficial in the setting of systolic HF where contractility is depressed. However, during diastolic HF [HFPEF (heart failure with preserved ejection fraction)], reducing the Ca^{2+} store is of less concern and enhancing Ca^{2+} extrusion by NCX1 may favourably improve diastolic function in these patients.

We also identified a PLM–NCX1 interaction in brain tissue, which may have important consequences for brain ischaemia. Previous study has confirmed the neuroprotective function of NCX, as knockout of NCX1, NCX2 and NCX3 resulted in augmented brain damage during ischaemia [48]. Furthermore, up-regulation of NCX1 and NCX3 have been shown to be neuroprotective in ischaemic pre-conditioning [49]. Similarly, in the heart, maintenance of low Ca^{2+} during ischaemia/reperfusion is known to be protective through forward-mode NCX1. Our present strategy of activation of NCX1 function without interference with NKA function may therefore be well suited for treating brain and cardiac ischaemia.

AUTHOR CONTRIBUTION

Pimthanya Wanichawan and Cathrine Rein Carlson conceived and co-ordinated the study and wrote the paper. Pimthanya Wanichawan, Tandekile Lubelwana Hafver, Marianne Lunde, Marita Martinsen and Cathrine Rein Carlson designed, performed and analysed the experiments shown in Figure 1–4 and Figure 6. Kjetil Hodne designed, performed and analysed the experiments shown in Figure 5. William Edward Louch, Ole Mathias Sejersted and Cathrine Rein Carlson provided technical assistance and contributed to the preparation of the Figures. All authors reviewed the results and approved the final version of the paper.

DECLARATION OF INTEREST

Pimthanya Wanichawan, Kjetil Hodne, Ole Mathias Sejersted and Cathrine Rein Carlson are partners on a patent application.

FUNDING

This work was supported by the Research Council of Norway, Norwegian National Health Association, Stiftelsen Kristian Gerhard Jebsen, Anders Jahre's Fund for the promotion of Science, the South-Eastern Norway Regional Health Authority [grant number 2016095], and the Simon Fougner Hartmanns family Fund, Denmark.

REFERENCES

1 Blaustein, M.P. and Lederer, W.J. (1999) Sodium/calcium exchange: its physiological implications. Physiol. Rev. **79**, 763–854 PubMed

2 Nicoll, D.A., Longoni, S. and Philipson, K.D. (1990) Molecular cloning and functional expression of the cardiac sarcolemmal Na^+–Ca^{2+} exchanger. Science **250**, 562–565 CrossRef PubMed

3 Lee, S.L., Yu, A.S. and Lytton, J. (1994) Tissue-specific expression of Na^+–Ca^{2+} exchanger isoforms. J. Biol. Chem. **269**, 14849–14852 PubMed

4 Nicoll, D.A., Quednau, B.D., Qui, Z., Xia, Y.R., Lusis, A.J. and Philipson, K.D. (1996) Cloning of a third mammalian Na^+–Ca^{2+} exchanger, NCX3. J. Biol. Chem. **271**, 24914–24921 CrossRef PubMed

5 Quednau, B.D., Nicoll, D. and Philipson, K.D. (1997) Tissue specificity and alternative splicing of the Na^+/Ca^{2+} exchanger isoforms NCX1, NCX2, and NCX3 in rat. Am. J. Physiol. **272**, C1250–C1261 PubMed

6 Li, Z., Nicoll, D.A., Collins, A., Hilgemann, D.W., Filoteo, A.G., Penniston, J.T., Weiss, J.N., Tomich, J.M. and Philipson, K.D. (1991) Identification of a peptide inhibitor of the cardiac sarcolemmal Na^+–Ca^{2+} exchanger. J. Biol. Chem. **266**, 1014–1020 PubMed

7 Hilge, M., Aelen, J. and Vuister, G.W. (2006) Ca^{2+} regulation in the Na^+/Ca^{2+} exchanger involves two markedly different Ca^{2+} sensors. Mol. Cell **22**, 15–25 CrossRef PubMed

8 Xue, X.H., Hryshko, L.V., Nicoll, D.A., Philipson, K.D. and Tibbits, G.F. (1999) Cloning, expression, and characterization of the trout cardiac Na^+/Ca^{2+} exchanger. Am. J. Physiol. **277**, C693–C700 PubMed

9 Wanichawan, P., Hafver, T.L., Hodne, K., Aronsen, J.M., Lunde, I.G., Dalhus, B., Lunde, M., Kvaloy, H., Louch, W.E., Tonnessen, T. et al. (2014) Molecular basis of calpain cleavage and inactivation of the sodium-calcium exchanger 1 in heart failure. J. Biol. Chem. **289**, 33984–33998 CrossRef PubMed

10 Wang, J., Zhang, X.Q., Ahlers, B.A., Carl, L.L., Song, J., Rothblum, L.I., Stahl, R.C., Carey, D.J. and Cheung, J.Y. (2006) Cytoplasmic tail of phospholemman interacts with the intracellular loop of the cardiac Na^+/Ca^{2+} exchanger. J. Biol. Chem. **281**, 32004–32014 CrossRef PubMed

11 Sweadner, K.J. and Rael, E. (2000) The FXYD gene family of small ion transport regulators or channels: cDNA sequence, protein signature sequence, and expression. Genomics **68**, 41–56 CrossRef PubMed

12 Ahlers, B.A., Zhang, X.Q., Moorman, J.R., Rothblum, L.I., Carl, L.L., Song, J., Wang, J., Geddis, L.M., Tucker, A.L., Mounsey, J.P. and Cheung, J.Y. (2005) Identification of an endogenous inhibitor of the cardiac Na^+/Ca^{2+} exchanger, phospholemman. J. Biol. Chem. **280**, 19875–19882 CrossRef PubMed

13 Feschenko, M.S., Donnet, C., Wetzel, R.K., Asinovski, N.K., Jones, L.R. and Sweadner, K.J. (2003) Phospholemman, a single-span membrane protein, is an accessory protein of Na,K-ATPase in cerebellum and choroid plexus. J. Neurosci. **23**, 2161–2169 PubMed

14 Presti, C.F., Jones, L.R. and Lindemann, J.P. (1985) Isoproterenol-induced phosphorylation of a 15-kilodalton sarcolemmal protein in intact myocardium. J. Biol. Chem. **260**, 3860–3867 PubMed

15 Zhang, X.Q., Qureshi, A., Song, J., Carl, L.L., Tian, Q., Stahl, R.C., Carey, D.J., Rothblum, L.I. and Cheung, J.Y. (2003) Phospholemman modulates Na^+/Ca^{2+} exchange in adult rat cardiac myocytes. Am. J. Physiol. Heart Circ. Physiol. **284**, H225–H233 CrossRef PubMed

16 Song, J., Zhang, X.Q., Ahlers, B.A., Carl, L.L., Wang, J., Rothblum, L.I., Stahl, R.C., Mounsey, J.P., Tucker, A.L., Moorman, J.R. and Cheung, J.Y. (2005) Serine 68 of phospholemman is critical in modulation of contractility, $[Ca^{2+}]_i$ transients, and Na^+/Ca^{2+} exchange in adult rat cardiac myocytes. Am. J. Physiol. Heart Circ. Physiol. **288**, H2342–H2354 CrossRef PubMed

17 Zhang, X.Q., Wang, J., Carl, L.L., Song, J., Ahlers, B.A. and Cheung, J.Y. (2009) Phospholemman regulates cardiac Na^+/Ca^{2+} exchanger by interacting with the exchanger's proximal linker domain. Am. J. Physiol. Cell Physiol. **296**, C911–C921 CrossRef PubMed

18 Zhang, X.Q., Ahlers, B.A., Tucker, A.L., Song, J., Wang, J., Moorman, J.R., Mounsey, J.P., Carl, L.L., Rothblum, L.I. and Cheung, J.Y. (2006) Phospholemman inhibition of the cardiac Na^+/Ca^{2+} exchanger: role of phosphorylation. J. Biol. Chem. **281**, 7784–7792 CrossRef PubMed

19 Song, Q., Pallikkuth, S., Bossuyt, J., Bers, D.M. and Robia, S.L. (2011) Phosphomimetic mutations enhance oligomerization of phospholemman and modulate its interaction with the Na/K-ATPase. J. Biol. Chem. **286**, 9120–9126 CrossRef PubMed

20 Bossuyt, J., Despa, S., Martin, J.L. and Bers, D.M. (2006) Phospholemman phosphorylation alters its fluorescence resonance energy transfer with the Na/K-ATPase pump. J. Biol. Chem. **281**, 32765–32773 CrossRef PubMed

21 Despa, S., Tucker, A.L. and Bers, D.M. (2008) Phospholemman-mediated activation of Na/K-ATPase limits $[Na]_i$ and inotropic state during β-adrenergic stimulation in mouse ventricular myocytes. Circulation **117**, 1849–1855 CrossRef PubMed

22 Boguslavskyi, A., Pavlovic, D., Aughton, K., Clark, J.E., Howie, J., Fuller, W. and Shattock, M.J. (2014) Cardiac hypertrophy in mice expressing unphosphorylatable phospholemman. Cardiovasc. Res. **104**, 72–82 CrossRef PubMed

23 Canzoniero, L.M., Rossi, A., Taglialatela, M., Amoroso, S., Annunziato, L. and Di Renzo, G. (1992) The Na^+–Ca^{2+} exchanger activity in cerebrocortical nerve endings is reduced in old compared to young and mature rats when it operates as a Ca^{2+} influx or efflux pathway. Biochim. Biophys. Acta **1107**, 175–178 CrossRef PubMed

24 Boscia, F., D'Avanzo, C., Pannaccione, A., Secondo, A., Casamassa, A., Formisano, L., Guida, N., Scorziello, A., Di Renzo, G. and Annunziato, L. (2013) New roles of NCX in glial cells: activation of microglia in ischemia and differentiation of oligodendrocytes. Adv. Exp. Med. Biol. **961**, 307–316 CrossRef PubMed

25 Pignataro, G., Tortiglione, A., Scorziello, A., Giaccio, L., Secondo, A., Severino, B., Santagada, V., Caliendo, G., Amoroso, S., Di Renzo, G. and Annunziato, L. (2004) Evidence for a protective role played by the Na^+/Ca^{2+} exchanger in cerebral ischemia induced by middle cerebral artery occlusion in male rats. Neuropharmacology **46**, 439–448 CrossRef PubMed

26 Louch, W.E., Stokke, M.K., Sjaastad, I., Christensen, G. and Sejersted, O.M. (2012) No rest for the weary: diastolic calcium homeostasis in the normal and failing myocardium. Physiology (Bethesda) **27**, 308–323 CrossRef PubMed

27 Song, J., Gao, E., Wang, J., Zhang, X.Q., Chan, T.O., Koch, W.J., Shang, X., Joseph, J.I., Peterson, B.Z., Feldman, A.M. and Cheung, J.Y. (2012) Constitutive overexpression of phosphomimetic phospholemman S68E mutant results in arrhythmias, early mortality, and heart failure: potential involvement of Na^+/Ca^{2+} exchanger. Am. J. Physiol. Heart Circ. Physiol. **302**, H770–H781 CrossRef PubMed

28 Frank, R. (1992) Spot-synthesis: an easy technique for the positionally addressable, parallel chemical synthesis on a membrane support. Tetrahedron **48**, 9217–9232 CrossRef

29 Frank, R. (2002) The SPOT-synthesis technique: synthetic peptide arrays on membrane supports-principles and applications. J. Immunol. Methods **267**, 13–26 CrossRef PubMed

30 Wanichawan, P., Louch, W.E., Hortemo, K.H., Austbo, B., Lunde, P.K., Scott, J.D., Sejersted, O.M. and Carlson, C.R. (2011) Full-length cardiac Na^+/Ca^{2+} exchanger 1 protein is not phosphorylated by protein kinase A. Am. J. Physiol. Cell Physiol. **300**, C989–C997 CrossRef PubMed

31 Zhang, X.Q., Wang, J., Song, J., Ji, A.M., Chan, T.O. and Cheung, J.Y. (2011) Residues 248–252 and 300–304 of the cardiac Na^+/Ca^{2+} exchanger are involved in its regulation by phospholemman. Am. J. Physiol. Cell Physiol. **301**, C833–C840 CrossRef PubMed

32 Cheung, J.Y., Zhang, X.Q., Song, J., Gao, E., Rabinowitz, J.E., Chan, T.O. and Wang, J. (2010) Phospholemman: a novel cardiac stress protein. Clin. Transl. Sci. **3**, 189–196 CrossRef PubMed

33 Nicoll, D.A., Ottolia, M., Goldhaber, J.I. and Philipson, K.D. (2013) 20 years from NCX purification and cloning: milestones. Adv. Exp. Med. Biol. **961**, 17–23 CrossRef PubMed

34 Matsuoka, S., Nicoll, D.A., He, Z. and Philipson, K.D. (1997) Regulation of cardiac Na^+–Ca^{2+} exchanger by the endogenous XIP region. J. Gen. Physiol. **109**, 273–286 CrossRef PubMed

35 Hilge, M., Aelen, J., Foarce, A., Perrakis, A. and Vuister, G.W. (2009) Ca^{2+} regulation in the Na^+/Ca^{2+} exchanger features a dual electrostatic switch mechanism. Proc. Natl. Acad. Sci. U.S.A. **106**, 14333–14338 CrossRef PubMed

36 Matsuoka, S., Nicoll, D.A., Hryshko, L.V., Levitsky, D.O., Weiss, J.N. and Philipson, K.D. (1995) Regulation of the cardiac Na^+–Ca^{2+} exchanger by Ca^{2+}: mutational analysis of the Ca^{2+}-binding domain. J. Gen. Physiol. **105**, 403–420 CrossRef PubMed

37 Ren, X., Nicoll, D.A., Galang, G. and Philipson, K.D. (2008) Intermolecular cross-linking of Na^+–Ca^{2+} exchanger proteins: evidence for dimer formation. Biochemistry **47**, 6081–6087 CrossRef PubMed

38 John, S.A., Ribalet, B., Weiss, J.N., Philipson, K.D. and Ottolia, M. (2011) Ca^{2+}-dependent structural rearrangements within Na^+–Ca^{2+} exchanger dimers. Proc. Natl. Acad. Sci. U.S.A. **108**, 1699–1704 CrossRef PubMed

39 Bossuyt, J., Despa, S., Han, F., Hou, Z., Robia, S.L., Lingrel, J.B. and Bers, D.M. (2009) Isoform specificity of the Na/K-ATPase association and regulation by phospholemman. J. Biol. Chem. **284**, 26749–26757 CrossRef PubMed

40 Khafaga, M., Bossuyt, J., Mamikonian, L., Li, J.C., Lee, L.L., Yarov-Yarovoy, V., Despa, S. and Bers, D.M. (2012) Na^+/K^+-ATPase E960 and phospholemman F28 are critical for their functional interaction. Proc. Natl. Acad. Sci. U.S.A. **109**, 20756–20761 CrossRef PubMed

41 Guo, K., Wang, X., Gao, G., Huang, C., Elmslie, K.S. and Peterson, B.Z. (2010) Amino acid substitutions in the FXYD motif enhance phospholemman-induced modulation of cardiac L-type calcium channels. Am. J. Physiol. Cell Physiol. **299**, C1203–C1211 CrossRef PubMed

42 Wang, X., Gao, G., Guo, K., Yarotskyy, V., Huang, C., Elmslie, K.S. and Peterson, B.Z. (2010) Phospholemman modulates the gating of cardiac L-type calcium channels. Biophys. J. **98**, 1149–1159 CrossRef PubMed

43 Zhang, X.Q., Wang, J., Song, J., Rabinowitz, J., Chen, X., Houser, S.R., Peterson, B.Z., Tucker, A.L., Feldman, A.M. and Cheung, J.Y. (2015) Regulation of L-type calcium channel by phospholemman in cardiac myocytes. J. Mol. Cell. Cardiol. **84**, 104–111 CrossRef PubMed

44 Cheung, J.Y., Zhang, X.Q., Song, J., Gao, E., Chan, T.O., Rabinowitz, J.E., Koch, W.J., Feldman, A.M. and Wang, J. (2013) Coordinated regulation of cardiac Na^+/Ca^{2+} exchanger and Na^+–K^+-ATPase by phospholemman (FXYD1). Adv. Exp. Med. Biol. **961**, 175–190 CrossRef PubMed

45 Swift, F., Birkeland, J.A., Tovsrud, N., Enger, U.H., Aronsen, J.M., Louch, W.E., Sjaastad, I. and Sejersted, O.M. (2008) Altered Na^+/Ca^{2+}-exchanger activity due to downregulation of Na^+/K^+-ATPase α_2-isoform in heart failure. Cardiovasc. Res. **78**, 71–78 CrossRef PubMed

46 Swift, F., Tovsrud, N., Sjaastad, I., Sejersted, O.M., Niggli, E. and Egger, M. (2010) Functional coupling of α_2-isoform Na^+/K^+-ATPase and Ca^{2+} extrusion through the Na^+/Ca^{2+}-exchanger in cardiomyocytes. Cell Calcium **48**, 54–60 CrossRef PubMed

47 Hasenfuss, G. and Pieske, B. (2002) Calcium cycling in congestive heart failure. J. Mol. Cell. Cardiol. **34**, 951–969 CrossRef PubMed

48 Molinaro, P., Cataldi, M., Cuomo, O., Viggiano, D., Pignataro, G., Sirabella, R., Secondo, A., Boscia, F., Pannaccione, A., Scorziello, A. et al. (2013) Genetically modified mice as a strategy to unravel the role played by the Na^+/Ca^{2+} exchanger in brain ischemia and in spatial learning and memory deficits. Adv. Exp. Med. Biol **961**, 213–222 CrossRef PubMed

49 Pignataro, G., Boscia, F., Esposito, E., Sirabella, R., Cuomo, O., Vinciguerra, A., Di Renzo, G. and Annunziato, L. (2012) NCX1 and NCX3: two new effectors of delayed preconditioning in brain ischemia. Neurobiol. Dis. **45**, 616–623 CrossRef PubMed

Received 22 January 2016/30 May 2016; accepted 31 May 2016
Accepted Manuscript online 31 May 2016, doi:10.1042/BCJ20160465